

CrossMark
click for updates

Cite this: DOI: 10.1039/c5ta10239a

Molecular surface functionalization to enhance the power output of triboelectric nanogenerators†

Sihong Wang,^{‡a} Yunlong Zi,^{‡a} Yu Sheng Zhou,^a Shengming Li,^a Fengru Fan,^b Long Lin^a and Zhong Lin Wang^{*ab}

Triboelectric nanogenerators (TENGs) have been invented as a new technology for harvesting mechanical energy, with enormous advantages. One of the major themes in their development is the improvement of the power output, which is fundamentally determined by the triboelectric charge density. Besides the demonstrated physical surface engineering methods to enhance this density, chemical surface functionalization to modify the surface potential could be a more effective and direct approach. In this paper, we introduced the method of using self-assembled monolayers (SAMs) to functionalize surfaces for the enhancement of TENGs' output. By using thiol molecules with different head groups to functionalize Au surfaces, the influence of head groups on both the surface potential and the triboelectric charge density was systematically studied, which reveals their direct correlation. With amine as the head group, the TENG's output power is enhanced by ~4 times. By using silane-SAMs with an amine head group to modify the silica surface, this approach is also demonstrated for insulating triboelectric layers in TENGs. This research provides an important route for the future research on improving TENGs' output through materials optimization.

Received 14th December 2015

Accepted 28th January 2016

DOI: 10.1039/c5ta10239a

www.rsc.org/MaterialsA

Introduction

As a huge energy reservoir in the environment that can be potentially utilized by human beings, mechanical energy is taking a more and more important role in satisfying the world's energy consumption.^{1–4} Besides the traditional technologies for harvesting mechanical energy on the basis of electromagnetics,^{5,6} electrostatics^{7,8} and piezoelectricity,^{9–11} triboelectric nanogenerators (TENGs)^{2,12–23} based on the conjunction of contact-electrification^{24–26} and electrostatic induction were invented and have been rapidly developed to be an extremely effective energy conversion technology, with the advantages of high power output and energy-conversion efficiency, low cost, abundant choice of materials, and wide range of applications. Similar to other energy conversion technologies such as photovoltaics^{27,28} and thermoelectrics,^{29,30} the improvement of the output power and the energy conversion efficiency is one of the major themes in the development of TENGs, which has been effectively achieved by new working mode establishment^{18,19,21} and rational structural designs.^{13,16,22,23} Besides, materials optimization is the other important route for this purpose. From the

materials' aspect, it has been shown that the performance figure-of-merit of TENGs is proportional to the square of the triboelectric charge density, which is the most important parameter to determine the power output.³¹ A previous research study has revealed that there is still huge room for improving the triboelectric charge density as well as output performances of TENGs under the structurally determined maximum charge density.³² Besides the physical surface engineering approaches for improving the triboelectric charge density,^{33,34} chemical surface functionalization would be a more direct and effective way, because the driving force for the contact electrification is closely related to the chemical potential difference between two surfaces.³⁵ Since the chemical potential of an organic material is mainly determined by its functional group,^{36,37} the surface potential could be effectively tuned by changing the functional groups exposed on the surface without changing the bulk material and its bulk properties.

According to the electronegativities of these functional groups, fluoro (–F) has the highest tendency to attract electrons, while amine (–NH₂) has the lowest tendency.^{38,39} Since there do exist perfluorinated materials (such as Teflon-series) that are all covered with the fluoro group to be the most triboelectrically negative choices, we only need to use chemical surface engineering approaches to make certain polymers terminated by amine for the best enhancement of triboelectric charge density. Among different surface engineering approaches, self-assembled monolayers (SAMs), which are the ordered molecular assemblies formed by the chemical

^aSchool of Materials Science and Engineering, Georgia Institute of Technology, Atlanta, GA 30332-0245, USA. E-mail: zhong.wang@mse.gatech.edu

^bBeijing Institute of Nanoenergy and Nanosystems, Chinese Academy of Sciences, Beijing, 100083, China

† Electronic supplementary information (ESI) available. See DOI: 10.1039/c5ta10239a

‡ These authors contributed equally to this work.

adsorption of an active surfactant on a solid surface, are important ones that are easily manufacturable and widely applicable to different surfaces.⁴⁰ Therefore, they can potentially serve as an effective chemical approach for improving the output performance of TENGs.

Here, we have utilized two types of self-assembled monolayers—thiols and silanes—to modify the surfaces of conductive and insulating materials, respectively. As a result, the triboelectric charges generated by the contact-electrification with a perfluorinated material—fluorinated ethylene propylene (FEP)—were improved effectively. By using different thiol molecules, the influence of head groups on the surface potential was systematically studied using scanning Kelvin probe microscopy (SKPM),^{41,42} which is in accordance with the influence on the surface charge density obtained from TENGs' output. It can be found that amine ($-\text{NH}_2$) is the most triboelectrically positive functional group that brings the largest enhancement to the generated charge density, while halogens (such as $-\text{Cl}$) are the most triboelectrically negative ones. The amine-functionalized surface is shown to be chemically stable during both a long period of time (over 90 days) and a large number of continuous operating cycles (over 100 000) to generate a similar triboelectric charge density. As a demonstration of the dielectric materials, the silica (SiO_2) surface was functionalized to be a lot more triboelectrically positive by using a silane molecule with amine as the head group. From this work, a clear surface engineering route is provided for the future research on the enhancement of TENGs' output performance from the materials' aspect.

Results and discussion

Among different classes of SAMs, the most extensively studied one is the absorption of alkanethiols ($\text{HS}(\text{CH}_2)_n\text{X}$) on the noble metals (such as gold, silver, copper, and palladium) with high affinities.⁴³ Due to the strong interaction with the sulfhydryl ($-\text{SH}$) group and the high quality of the film, gold is the most widely used substrate for the alkanethiol SAMs.^{43–45} Because the head group ($-\text{X}$) in alkanethiol molecules can be almost any functional groups, we can use this SAM chemistry to modify the Au surface with different desired functional groups to give different surface potentials, and thus differently enhanced triboelectric charge density from contact-electrification. The fabrication of such SAM-modified surfaces starts from the deposition of Au thin films (with a thickness of 100 nm) on Kapton substrates (Fig. 1a(I and II)), which are flexible and light in weight. Then, these substrates were immersed in different thiol solutions all with a concentration of 10 mM, for 12 hours (Fig. 1a(III)). Next, these Kapton-based films were utilized to fabricate contact-separation mode TENGs, in which the functionalized Au surface serves as both the triboelectric surface and the electrode on one side. On the other side, a fluorinated ethylene propylene (FEP) film with a thickness of 50 μm is purposely chosen as the counter triboelectric surface due to its most negative triboelectric polarity. A layer of a Cu thin film was deposited at the back as the corresponding electrode. Both the triboelectric films were laminated on acrylic plates to ensure flat

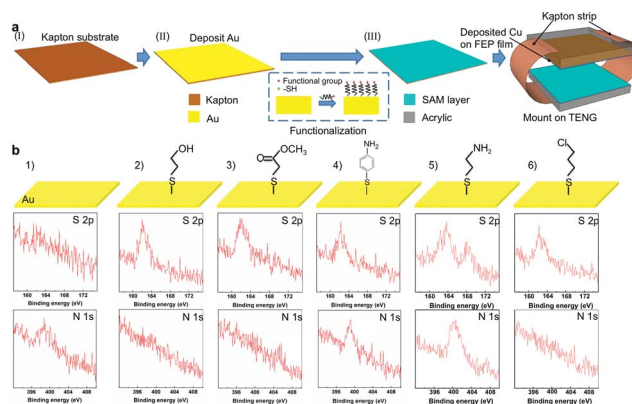


Fig. 1 (a) Fabrication process of TENGs from the thiol-SAM functionalized Au films. (b) Molecular structures of the thiols and corresponding XPS characterization of the functionalized surfaces.

surfaces. A pair of bent Kapton strips were utilized to connect and support the two plates, which bring them into the separation state when external pressing force is withdrawn.

From this thiol-based SAM functionalization process, four different functional groups are brought onto the Au surface: hydroxyl ($-\text{OH}$), ester ($-\text{COOCH}_3$), amine ($-\text{NH}_2$) and chloro ($-\text{Cl}$), among which amine should be the one to give the most significant enhancement to the triboelectric charge density from the contact-electrification with FEP. The molecules utilized to form SAMs with these functional groups are shown in Fig. 1b(2)–(6), in which the functionalization of amine is realized by two different molecules: 4-aminothiophenol (4) and cysteamine hydrochloride (5). In the following part in this paper, these numbers are used to represent these molecules, while #1 represents the pristine Au surface. The formation of these SAMs on the Au surfaces was characterized by X-ray photoelectron spectroscopy (XPS), together with the pristine Au surface as a comparison. As shown in Fig. 1b, the S-2p peak appears in all the five thiol-functionalized surfaces but is not observed in the pristine Au surface. This clearly shows the successful assembly of the thiol molecules on these surfaces after the functionalization step. Since the enhancement of the triboelectric charge density is expected to be realized by the amine group that is introduced by thiol molecules #4 & #5, we

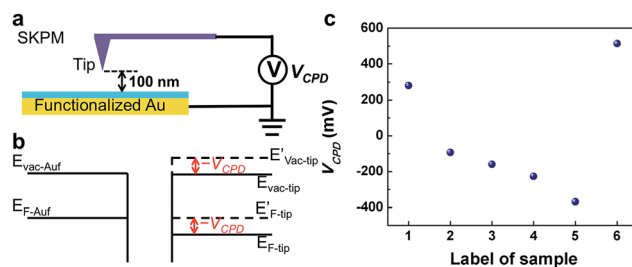


Fig. 2 SKPM characterization of the thiol-modified Au surfaces. (a) Experimental setup of the SKPM. (b) Working mechanism of the SKPM. (c) Measurement results of using SKPM to characterize the chemical potentials of the functionalized Au.

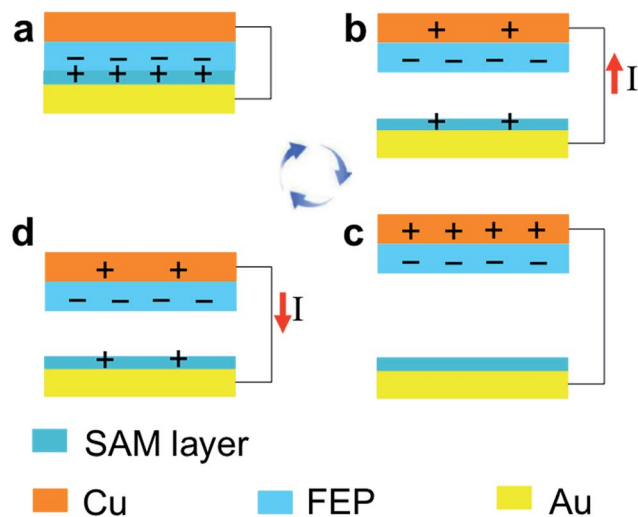


Fig. 3 Working mechanism of the TENG, including (a) the full contact status, (b) the status of being separated, (c) full separation status, and (d) the status of being in contact.

also monitored the appearance of the N-1s peak around 400 eV. As can be seen from Fig. 1b, the existence of the amine group only on the surfaces of #4 & #5 is verified.

The change of the surface potential by these SAMs with different functional groups was characterized using a scanning Kelvin probe microscope (SKPM).^{41,42} As shown in Fig. 2a, the tip of the microscope approaches the functionalized Au surface with a distance of 100 nm during the measurement. The Au surface is grounded. A voltage is applied to nullify the potential difference existing between the Fermi levels of the tip and the functionalized Au. Therefore, this voltage is taken as the contact potential difference (V_{CPD}). According to this working principle of SKPM, if the Fermi level of the functionalized Au surface (E_{F-AuF}) is higher than the Fermi level of the tip (E_{F-tip}), a negative V_{CPD} needs to be applied onto the tip to match the two Fermi levels (Fig. 2b). Thus, a more negative value of V_{CPD} given by the SKPM represents a higher Fermi level of the detected surface, and *vice versa*. The V_{CPD} values obtained from all these surfaces of #1 to #6 are plotted in Fig. 2c. For all these surfaces, the results from the scanned areas have standard deviations smaller than 5 mV, which shows the uniform functionalization across the surfaces. Compared to the pristine Au surface #1, the functional groups of hydroxyl (#2), ester (#3) and amine (#4) & (#5) all increase the surface potential, with the largest increase brought by amine and the smallest increase by hydroxyl, which shows that these functional groups should all give the surface a higher tendency in generating positive triboelectric charges through the contact electrification. Between these two amined-ended thiol molecules #4 & #5, molecule #5 leads to a larger increase in the surface chemical potential. The difference may come from the relatively higher electronegativity of the phenylene ($-C_6H_4-$) group than that of the ethylene ($-CH_2-$) group.³⁹ Therefore, the functionalization of these three functional groups should make the surface more triboelectrically positive. In contrast, the higher V_{CPD} value measured from the surface #6 indicates that the chloro group serves to lower the surface

potential, giving it a stronger attraction to electrons. These results clearly show that the functionalization of the surface can effectively alter the surface potential, which is in accordance with the expectation of the electronegativities of these functional groups.

Because of the basic working principle of the contact-separation mode TENG, a higher triboelectric surface charge density will generate a higher amount of charges transferring through the external load in each operation cycle. The schemes of its operation principle are shown in Fig. 3. When the two triboelectric surfaces (*i.e.* functionalized Au and FEP) get into contact under external mechanical agitation, opposite triboelectric charges will be generated on the two surfaces with the same density: positive charges on the functionalized Au surface and negative charges on FEP. Upon releasing, the two oppositely charged surfaces start to get separated from each other, inducing a potential difference between the two electrodes (*i.e.* Cu and functionalized Au). This potential difference will drive electrons to flow from the Cu electrode to the functionalized Au (Fig. 3b). When the separation between the two layers reaches the maximum, almost all the positive triboelectric charges on the functionalized Au will be neutralized, so that the density of positive charges on the Cu electrode equals to that on the Au electrode for the electrostatic equilibrium (Fig. 3c). Subsequently, when the two layers are pressed to approach each other again, the reversed potential difference between the two electrodes will build, which leads to the back flow of all the transferred electrons from the functionalized Au to the Cu electrode (Fig. 3d). From the previous fundamental study on the contact-separation mode TENG, a higher triboelectric surface charge density will produce not only an equally higher amount of transferred charges in the external circuit (and thus a higher

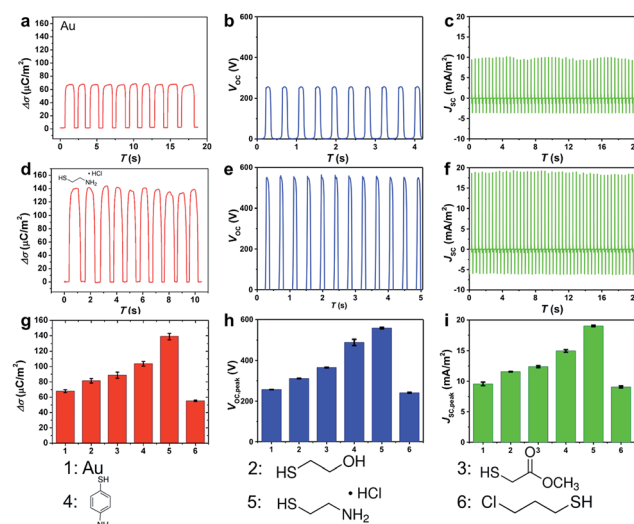


Fig. 4 Output performance of the TENGs with pristine (#1) and functionalized Au (#2–6) surfaces. (a–c) and (d–f) show the measured transferred charge density ($\Delta\sigma$), the open-circuit voltage (V_{OC}) and short-circuit current density (J_{SC}) of the #1 and #5 TENGs, respectively. (g–i) show the comparisons of the transferred charge density, open-circuit voltage and short-circuit current density of all the 6 TENGs.

short-circuit current density), but also a larger open-circuit voltage.

To systematically characterize the influence of the assembled functional groups on the triboelectric charge density and the output performances of TENGs, the short-circuit transferred charge density ($\Delta\sigma$), the open-circuit voltage (V_{OC}), and the short-circuit current density (J_{SC}) were measured for the TENGs fabricated from all the 6 differently functionalized Au surfaces (#1 – #6). As shown in Fig. 4a and b, the TENG fabricated from the pristine Au (#1) gives a $\Delta\sigma$ of $\sim 68 \mu\text{C m}^{-2}$ (under the periodical pressing by human hand), and a V_{OC} of $\sim 270 \text{ V}$ (under the triggering by a linear motor). This $\Delta\sigma$ should represent the triboelectric charge density generated by the pristine Au surface. Under agitation from a mechanical shaker with a frequency of $\sim 2.5 \text{ Hz}$, the TENG generates a J_{SC} of $\sim 9 \text{ mA m}^{-2}$. After being functionalized by the thiol molecules, the best enhancement of TENG's output comes from the surface #5, which is covered with the SAM of cysteamine hydrochloride with amine as the head group. The $\Delta\sigma$ (*i.e.* the triboelectric charge density) was increased to $\sim 140 \mu\text{C m}^{-2}$ (Fig. 4d). The V_{OC} and the J_{SC} reached $\sim 560 \text{ V}$ (Fig. 4e) and $\sim 18.5 \text{ mA m}^{-2}$ (Fig. 4f), respectively. This is a significant enhancement to the TENG's output by the functionalization of the amine group. The groups of hydroxyl (#2), ester (#3), and amine from 4-aminothiophenol (#4) all give an enhancement to the TENG's output with relatively smaller extents (Fig. 4g–i), which comes from the enhancement of the triboelectric charge density. The enhancement from these functional group ranks from high to low as: amine from 4-aminothiophenol (#4), ester (#3) and hydroxyl (#2). This is in line with the increase of the surface potential by these function groups shown in Fig. 2c as directly measured by the SKPM. Differently, the functionalization of the chloro functional group (#6) leads to a slight decrease of the TENG's output compared to the pristine Au, which should result from the smaller triboelectric charge density because of the decrease of the surface potential. The change of the triboelectric charge density by these functional groups is in accordance with the change of the surface chemical potentials through the self-assembly of these functional groups.

For the long-term applications of the enhanced triboelectric charge density by the SAM functionalization, both the time-dependent and the operation-dependent stabilities have been studied. For the time-dependent stability, the amine-

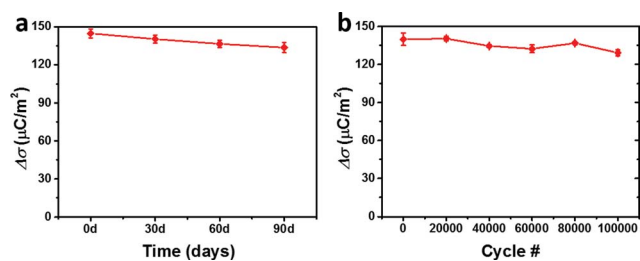


Fig. 5 Stability of the enhanced TENG output from the amine-group functionalized Au surface. (a) Time-dependent stability. (b) Operation-dependent stability.

functionalized surface was kept in air for over 90 days, and the charge transfer produced by the TENG was measured every 30 days to monitor the change of the triboelectric charge density. As shown in Fig. 5a, the triboelectric charge density only decreased from $\sim 140 \mu\text{C m}^{-2}$ to $\sim 130 \mu\text{C m}^{-2}$ in the time period of 90 days. This slight decrease should come from the oxidation of the thiol molecules during the exposure to air.^{44,46} Besides, the TENG is also tested under continuous operation cycles to reflect the stability of the SAM under repeated mechanical contact/friction. As can be seen from Fig. 5b, the triboelectric charge density remained at the level around $\sim 140 \mu\text{C m}^{-2}$ during the 100 000 operation cycles. This group of stability tests has confirmed the practicability of using the SAM to enhance the TENGs' output for long-term applications.

Besides the functionalization of a conductive surface (Au) as one triboelectric layer, we further used SiO_2 to demonstrate the applicability of this method for insulating triboelectric surfaces. As shown in Fig. 6a, a layer of SiO_2 was deposited by plasma-enhanced chemical vapor deposition (PECVD) on top of a glass slide as the substrate, with a Ti film in between serving as both the adhesion layer and the electrode on this side. Then, a silane molecule—(3-aminopropyl)triethoxysilane (APTES)— that has amine as the head group was used to form a SAM based on 3 Si–O bonds for each molecule.⁴⁷ The XPS results (Fig. S1†) of the N-1s peak from the SiO_2 samples before and after the functionalization clearly show that the amine group has been introduced onto the surface. The amine group is expected to increase the surface chemical potential of the SiO_2 and thus to promote its tendency to generate positive triboelectric charges. Subsequently, a TENG was fabricated from it, with a Cu-deposited FEP film on a glass slide as the counter layer. In this structure, two acrylic sheets work with four springs to ensure the separation between the two layers without external pressing force. With a pristine SiO_2 surface in the TENG, the $\Delta\sigma$, the V_{OC} , and the J_{SC}

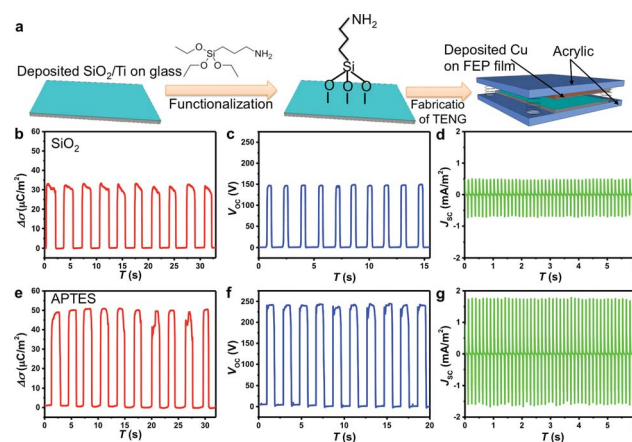


Fig. 6 SAM surface functionalization of SiO_2 as the triboelectric layer in TENGs to enhance the output performance. (a) Fabrication process and (b–g) output performances of the TENGs with pristine and functionalized silica (10% APTES in volume ratio). (b–d) and (e–g) show the measured charge density, the open-circuit voltage and the short-circuit current density of TENGs with the pristine and functionalized silica, respectively.

are only $\sim 34 \mu\text{C m}^{-2}$, $\sim 150 \text{ V}$ and $\sim 0.7 \text{ mA m}^{-2}$, respectively. After the functionalization in APTES solution of 10% concentration, the chemical potential of the SiO_2 gets higher and thus could generate more triboelectric charges through the contact-electrification with FEP. As a result, the $\Delta\sigma$, the V_{OC} , and the J_{SC} produced by the TENG were increased to $\sim 51 \mu\text{C m}^{-2}$, $\sim 240 \text{ V}$ and $\sim 1.75 \text{ mA m}^{-2}$, respectively. Through comparing with the TENG fabricated from the film functionalized by APTES of 1% concentration (Fig. S2†), we can find that a higher concentration of APTES gives a better improvement in the triboelectric charge density.

Conclusions

In this paper, we have demonstrated the methodology of chemical surface functionalization for the enhancement of TENGs' output performance through achieving a higher triboelectric charge density. Here, the functionalization is achieved by the self-assembled monolayers (SAMs)—thiol molecules for conductive surfaces (Au) and silane molecules for dielectric surfaces (SiO_2). It is shown that the influence on the triboelectric charge density is mainly determined by the type of head group of the SAMs through altering the surface chemical potential as revealed by the SKPM. Through using molecules with amine as the head group, the performance of both the Au-based TENG and SiO_2 -based TENG has been significantly improved. The SAM-based methodology developed in this paper is simple in operation, very effective, stable with time, and widely applicable to different materials. In the future research, a more significant enhancement could be achieved by using molecules with head groups of lower electronegativity for the positive side and higher electronegativity for the negative side, and molecules with longer chains to further minimize the influence from the substrate. By combining the chemical approach with physical approaches (such as introducing nanostructures) to modify surfaces, there could be a gigantic enhancement of the TENGs' output performance. This research provides an important direction for the future research on improving TENGs' output through materials optimization.

Experimental

TENG fabrication and measurements

To fabricate the first type of TENG with Au surfaces, the 100 nm Au films were first deposited on six $4.5 \text{ cm} \times 4.5 \text{ cm}$ Kapton substrates by using an e-beam evaporator. For #2–6 samples, the Au surfaces were functionalized (see below). The 100 nm Cu electrodes were deposited on six pieces of FEP film of the same size. And then all the Kapton films with Au surfaces and the FEP films with Cu electrodes were laminated on acrylic boards with polydimethylsiloxane (PDMS) as the adhesive layer. The Au and FEP surfaces were made to face each other to be triboelectric pairs. Two Kapton strips were installed on the two sides of the acrylic boards to let the TENG to be hold at the separation status without any mechanical pressure.

To fabricate the second type of TENG with SiO_2 surfaces, the 100 nm Ti film was first deposited on three $5 \text{ cm} \times 7.5 \text{ cm}$ glass

slides by e-beam evaporation, and then the SiO_2 films were deposited by a plasma-enhanced chemical vapor deposition (PECVD) method. For two of the samples, the SiO_2 surfaces were functionalized (see below). The 100 nm Cu electrodes were deposited on three pieces of FEP film of the same size by a physical vapor deposition method. And then all the glass slides with Ti/ SiO_2 surfaces and the FEP films with Cu electrodes were laminated on acrylic boards with PDMS as the binder. The SiO_2 and FEP surfaces were made to face each other to be triboelectric pairs. Four springs were installed on the four corners of the acrylic boards to let the TENG to be held at the separation status without any mechanical pressure.

Surface functionalization

Before functionalization, all the Au films deposited on the Kapton substrates and SiO_2/Ti films deposited on the glass slides were first ultrasonically cleaned with ethanol, isopropyl alcohol and acetone, and then these substrates were cleaned with O_2 plasma for 2 min. And then five of the Kapton substrates were immersed in 10 mM different thiol solutions in ethanol for 12 hours. The thiols used included 2-mercaptoethanol (#2), methyl thioglycolate (#3), 4-aminothiophenol (#4), cysteamine hydrochloride (#5) and 3-chloro-1-propanethiol (#6). Two of the glass slides were immersed in 1% and 10% (both in volume ratio) APTES solutions in ethanol for 12 hours, respectively.

XPS and SKPM characterization

To prepare samples for XPS and SKPM, the Au or Ti/ SiO_2 films were first deposited on Si substrates, and then the same functionalization process was performed on these substrates. The XPS spectra of these samples were collected through a Thermal K-Alpha XPS system. The SKPM surface potentials were collected by using tapping-mode scanning above the surfaces with the same Si/Pt conductive probe and identical settings.

Acknowledgements

The research was supported by the Hightower Chair foundation, National Natural Science Foundation of China (Grant No. 51432005) and the 'thousands talents' program for pioneer researcher and his innovation team, China.

Notes and references

- 1 Z. L. Wang and J. H. Song, Piezoelectric nanogenerators based on zinc oxide nanowire arrays, *Science*, 2006, **312**(5771), 242–246.
- 2 Z. L. Wang, Triboelectric Nanogenerators as New Energy Technology for Self-Powered Systems and as Active Mechanical and Chemical Sensors, *ACS Nano*, 2013, **7**(11), 9533–9557.
- 3 J. M. Donelan, Q. Li, V. Naing, J. A. Hoffer, D. J. Weber and A. D. Kuo, Biomechanical energy harvesting: generating electricity during walking with minimal user effort, *Science*, 2008, **319**(5864), 807–810.

- 4 L. C. Rome, L. Flynn, E. M. Goldman and T. D. Yoo, Generating electricity while walking with loads, *Science*, 2005, **309**(5741), 1725–1728.
- 5 S. P. Beeby, R. N. Torah, M. J. Tudor, P. Glynne-Jones, T. O'Donnell, C. R. Saha and S. Roy, A micro electromagnetic generator for vibration energy harvesting, *J. Micromech. Microeng.*, 2007, **17**(7), 1257–1265.
- 6 I. Sari, T. Balkan and H. Kulah, An electromagnetic micro power generator for wideband environmental vibrations, *Sens. Actuators, A*, 2008, **145**, 405–413.
- 7 P. D. Mitcheson, P. Miao, B. H. Stark, E. M. Yeatman, A. S. Holmes and T. C. Green, MEMS electrostatic micropower generator for low frequency operation, *Sens. Actuators, A*, 2004, **115**(2–3), 523–529.
- 8 Y. Suzuki, D. Miki, M. Edamoto and M. Honzumi, A MEMS electret generator with electrostatic levitation for vibration-driven energy-harvesting applications, *J. Micromech. Microeng.*, 2010, **20**(10), 104002.
- 9 Y. Qin, X. D. Wang and Z. L. Wang, Microfibre-nanowire hybrid structure for energy scavenging, *Nature*, 2008, **451**(7180), 809–813.
- 10 X. D. Wang, J. H. Song, J. Liu and Z. L. Wang, Direct-current nanogenerator driven by ultrasonic waves, *Science*, 2007, **316**(5821), 102–105.
- 11 Y. Qi, J. Kim, T. D. Nguyen, B. Lisko, P. K. Purohit and M. C. McAlpine, Enhanced Piezoelectricity and Stretchability in Energy Harvesting Devices Fabricated from Buckled PZT Ribbons, *Nano Lett.*, 2011, **11**(3), 1331–1336.
- 12 F. R. Fan, Z. Q. Tian and Z. L. Wang, Flexible triboelectric generator!, *Nano Energy*, 2012, **1**(2), 328–334.
- 13 S. H. Wang, L. Lin and Z. L. Wang, Nanoscale Triboelectric-Effect-Enabled Energy Conversion for Sustainably Powering Portable Electronics, *Nano Lett.*, 2012, **12**(12), 6339–6346.
- 14 B. Meng, W. Tang, X. S. Zhang, M. D. Han, W. Liu and H. X. Zhang, Self-powered flexible printed circuit board with integrated triboelectric generator, *Nano Energy*, 2013, **2**(6), 1101–1106.
- 15 S. Kim, M. K. Gupta, K. Y. Lee, A. Sohn, T. Y. Kim, K. S. Shin, D. Kim, S. K. Kim, K. H. Lee, H. J. Shin, D. W. Kim and S. W. Kim, Transparent Flexible Graphene Triboelectric Nanogenerators, *Adv. Mater.*, 2014, **26**(23), 3918–3925.
- 16 L. Lin, S. H. Wang, Y. N. Xie, Q. S. Jing, S. M. Niu, Y. F. Hu and Z. L. Wang, Segmentally Structured Disk Triboelectric Nanogenerator for Harvesting Rotational Mechanical Energy, *Nano Lett.*, 2013, **13**(6), 2916–2923.
- 17 Z. H. Lin, G. Cheng, L. Lin, S. Lee and Z. L. Wang, Water-Solid Surface Contact Electrification and its Use for Harvesting Liquid-Wave Energy, *Angew. Chem., Int. Ed.*, 2013, **52**(48), 12545–12549.
- 18 S. H. Wang, L. Lin, Y. N. Xie, Q. S. Jing, S. M. Niu and Z. L. Wang, Sliding-Triboelectric Nanogenerators Based on In-Plane Charge-Separation Mechanism, *Nano Lett.*, 2013, **13**(5), 2226–2233.
- 19 Y. Yang, H. L. Zhang, J. Chen, Q. S. Jing, Y. S. Zhou, X. N. Wen and Z. L. Wang, Single-Electrode-Based Sliding Triboelectric Nanogenerator for Self-Powered Displacement Vector Sensor System, *ACS Nano*, 2013, **7**(8), 7342–7351.
- 20 Y. F. Hu, J. Yang, S. M. Niu, W. Z. Wu and Z. L. Wang, Hybridizing Triboelectrification and Electromagnetic Induction Effects for High-Efficient Mechanical Energy Harvesting, *ACS Nano*, 2014, **8**(7), 7442–7450.
- 21 S. H. Wang, Y. N. Xie, S. M. Niu, L. Lin and Z. L. Wang, Freestanding Triboelectric-Layer-Based Nanogenerators for Harvesting Energy from a Moving Object or Human Motion in Contact and Non-contact Modes, *Adv. Mater.*, 2014, **26**(18), 2818–2824.
- 22 Y. N. Xie, S. H. Wang, S. M. Niu, L. Lin, Q. S. Jing, J. Yang, Z. Y. Wu and Z. L. Wang, Grating-Structured Freestanding Triboelectric-Layer Nanogenerator for Harvesting Mechanical Energy at 85% Total Conversion Efficiency, *Adv. Mater.*, 2014, **26**(38), 6599–6607.
- 23 G. Zhu, J. Chen, T. J. Zhang, Q. S. Jing and Z. L. Wang, Radial-arrayed rotary electrification for high performance triboelectric generator, *Nat. Commun.*, 2014, **5**, 3426.
- 24 R. G. Horn and D. T. Smith, Contact Electrification and Adhesion between Dissimilar Materials, *Science*, 1992, **256**(5055), 362–364.
- 25 L. S. McCarty and G. M. Whitesides, Electrostatic charging due to separation of ions at interfaces: contact electrification of ionic electrets, *Angew. Chem., Int. Ed.*, 2008, **47**(12), 2188–2207.
- 26 H. T. Baytekin, A. Z. Patashinski, M. Branicki, B. Baytekin, S. Soh and B. A. Grzybowski, The Mosaic of Surface Charge in Contact Electrification, *Science*, 2011, **333**(6040), 308–312.
- 27 B. Oregan and M. Gratzel, A Low-Cost, High-Efficiency Solar-Cell Based on Dye-Sensitized Colloidal TiO₂ Films, *Nature*, 1991, **353**(6346), 737–740.
- 28 W. U. Huynh, J. J. Dittmer and A. P. Alivisatos, Hybrid nanorod-polymer solar cells, *Science*, 2002, **295**(5564), 2425–2427.
- 29 R. Venkatasubramanian, E. Siivola, T. Colpitts and B. O'Quinn, Thin-film thermoelectric devices with high room-temperature figures of merit, *Nature*, 2001, **413**(6856), 597–602.
- 30 A. I. Hochbaum, R. K. Chen, R. D. Delgado, W. J. Liang, E. C. Garnett, M. Najarian, A. Majumdar and P. D. Yang, Enhanced thermoelectric performance of rough silicon nanowires, *Nature*, 2008, **451**(7175), 163–167.
- 31 Y. Zi, S. Niu, J. Wang, Z. Wen, W. Tang and Z. L. Wang, Standards and figure-of-merits for quantifying the performance of triboelectric nanogenerators, *Nat. Commun.*, 2015, **6**, 8376.
- 32 S. H. Wang, Y. N. Xie, S. M. Niu, L. Lin, C. Liu, Y. S. Zhou and Z. L. Wang, Maximum Surface Charge Density for Triboelectric Nanogenerators Achieved by Ionized-Air Injection: Methodology and Theoretical Understanding, *Adv. Mater.*, 2014, **26**(39), 6720–6728.
- 33 F. R. Fan, L. Lin, G. Zhu, W. Z. Wu, R. Zhang and Z. L. Wang, Transparent Triboelectric Nanogenerators and Self-Powered Pressure Sensors Based on Micropatterned Plastic Films, *Nano Lett.*, 2012, **12**(6), 3109–3114.

- 34 G. Zhu, Z. H. Lin, Q. S. Jing, P. Bai, C. F. Pan, Y. Yang, Y. S. Zhou and Z. L. Wang, Toward Large-Scale Energy Harvesting by a Nanoparticle-Enhanced Triboelectric Nanogenerator, *Nano Lett.*, 2013, **13**(2), 847–853.
- 35 J. Lowell and A. C. Roseinnes, Contact Electrification, *Adv. Phys.*, 1980, **29**(6), 947–1023.
- 36 K. Oura, *Surface Science: An Introduction*, Springer, Berlin, New York, 2003, p xii, p. 440.
- 37 W. C. Lin, S. H. Lee, M. Karakachian, B. Y. Yu, Y. Y. Chen, Y. C. Lin, C. H. Kuo and J. J. Shyue, Tuning the surface potential of gold substrates arbitrarily with self-assembled monolayers with mixed functional groups, *Phys. Chem. Chem. Phys.*, 2009, **11**(29), 6199–6204.
- 38 J. E. Huheey, Electronegativity of Groups, *J. Phys. Chem.*, 1965, **69**(10), 3284–3291.
- 39 J. E. Huheey, Electronegativity of Multiply Bonded Groups, *J. Phys. Chem.*, 1966, **70**(7), 2086–2092.
- 40 A. Ulman, Formation and structure of self-assembled monolayers, *Chem. Rev.*, 1996, **96**(4), 1533–1554.
- 41 W. Melitz, J. Shen, A. C. Kummel and S. Lee, Kelvin probe force microscopy and its application, *Surf. Sci. Rep.*, 2011, **66**(1), 1–27.
- 42 Y. S. Zhou, S. H. Wang, Y. Yang, G. Zhu, S. M. Niu, Z. H. Lin, Y. Liu and Z. L. Wang, Manipulating Nanoscale Contact Electrification by an Applied Electric Field, *Nano Lett.*, 2014, **14**(3), 1567–1572.
- 43 J. C. Love, L. A. Estroff, J. K. Kriebel, R. G. Nuzzo and G. M. Whitesides, Self-assembled monolayers of thiolates on metals as a form of nanotechnology, *Chem. Rev.*, 2005, **105**(4), 1103–1169.
- 44 C. Vericat, M. E. Vela, G. Benitez, P. Carro and R. C. Salvarezza, Self-assembled monolayers of thiols and dithiols on gold: new challenges for a well-known system, *Chem. Soc. Rev.*, 2010, **39**(5), 1805–1834.
- 45 C. Vericat, M. E. Vela, G. A. Benitez, J. A. M. Gago, X. Torrelles and R. C. Salvarezza, Surface characterization of sulfur and alkanethiol self-assembled monolayers on Au(111), *J. Phys.: Condens. Matter*, 2006, **18**(48), R867–R900.
- 46 S. Oae and J. T. Doi, *Organic Sulfur Chemistry*. CRC Press, Boca Raton, 1991, p. v.
- 47 J. H. Moon, J. W. Shin, S. Y. Kim and J. W. Park, Formation of uniform aminosilane thin layers: an imine formation to measure relative surface density of the amine group, *Langmuir*, 1996, **12**(20), 4621–4624.